Investigation of Planetary Gearbox Vibration Signal Characteristics and Failure Diagnosis Using Time-Spectral Kurtosis (TSK) and Ensemble Empirical Mode Decomposition (EEMD)

T- Bensana*, M-FNIDES*, L- BOURAGBI** and M-MIHOUB***

Keywords: planetary gearbox, vibratory diagnostics, Second-generation wavelet (SGW), ensemble empirical mode decomposition (EEMD), timespectral kurtosis (TSK).

ABSTRACT

Gears are an indispensable element of industrial equipment and power transmission in a wide range of manufacturing machinery. When faults occur on one or more gear teeth, the performance of the gear train deteriorates and the efficiency decreases. Vibration signal processing and analysis is one of the best preferred means to diagnose the planetary gearbox fault, but Vibration signal of gears is often submerged in a large amount of noise, leading to the decrease of fault diagnosis accuracy. In order to determine the faulty feature frequency of weak gear signals, a hybrid fault diagnosis method of planetary gear based on (SGW), Second-generation wavelet ensemble empirical mode decomposition (EEMD) and Time-Spectral Kurtosis (TSK) is proposed in this paper. Firstly, SGW denoising is employed to filter the initial signal then extract the signal of interest from the background noise. Next, decompose the filtered signal into IMFs and reduce modal aliasing using the EEMD approach. After that, the correlation coefficient and TSK are used to identify the faulty IMFs, which are subsequently used to reconstruct the last signal. Finally, the envelope spectrum of the reconstructed signal is used to detect the characteristic frequency. The results can ensure that characteristics of gear failures are included in the selected IMFs and confirm the effectiveness and superiority of the proposed adaptive method in gear fault diagnosis.

Paper Received February, 2025. Revised March, 2025. Accepted March, 2025. Author for Correspondence: T- Bensana

INTRODUCTION

Planetary gearboxes are usually used in aerospace, automotive and heavy manufacturing applications to derive benefits from their big transmission ratio, solid load-bearing capacity and great transmission effectiveness (J.Mc et al., 2002). Nevertheless these benefits, planetary gearboxes frequently experience gear tooth damage, such as fatigue cracks and missing teeth, due to the demanding operating conditions of heavy duty and intense impact load (F. Chaari et al., 2006). The identification of gearbox faults is critically significant and has been researched for numerous decades. A notable feature of gearbox malfunctions is their propensity to produce vibration signals characterized by amplitude and/or phase variation, the rise in sideband components surrounding the associated meshing frequencies and their harmonics (Upadhyay et al., 2017; Iatsenko et al., 2015). Consequently, feature extraction-based processing techniques continue to be crucial in the field of gear malfunction diagnostics. Time-Frequency Analysis (Lei et al., 2020; F. Li et al., 2018). Wavelet Transform (WT) (Yu, G et al., 2020; J. Pan et al., 2008; S. Chen et al., 2018). Spectral Kurtosis (SK) (Qin et al., 2019; Elforjani et al., 2018; Braun et al., 1986). Empirical Mode Decomposition (EMD) Prediction models (Wang et al., 2024; Ta-Jen Peng et al., 2024). Variational Mode Decomposition (VMD) (Xuejun Chen et al., 2019) and other signal processing techniques have been used in gear defect feature extraction. Sparse decomposition (SD) exhibits better feature extraction performance when compared to the aforementioned techniques. By choosing a small number of atoms from a suitable dictionary, SD can represent the fault feature signal sparsely. This technique has been effectively used in the diagnosis of gear faults (Cheng et al., 2008; Dragomiretskiy et al., 2014). Adaptive signal analysis techniques for non-stationary signals have garnered a lot of attention lately. These

^{*} Higher Normal School of Technological Education of Skikda, Azzaba Skikda, Algeria

^{**} University of 20th August 1955-Skikda, Department of Process Engineering, Skikda, Algeria.

^{***} Tissemsilt University, Tissemsilt, Algeria

techniques can adaptively break down a complex signal into several modes based on the signal's inherent characteristics and offer strong instruments for diagnosing gear faults and extracting periodic impulses. For instance, empirical mode decomposition (EMD) has been extensively researched and used in the identification of mechanical faults (L. Hui et al., 2006; Z. P. Feng et al., 2005). Nevertheless, the mode mixing issue is a significant liability. As a result, the ensemble EMD (EEMD) and other enhanced EMD techniques are introduced to mitigate the mode mixing issue in the EMD and have been extensively utilized for rotating machinery defect diagnosis (Amarnath et al., 2016; Smith et al., 2005). Mode mixing and overdecomposition are two issues brought on by background noise that impair these techniques' processing capabilities. In the field of signal processing, the issue of signal denoising has always been the focus of attention. Examining existing wavelet-based denoising techniques, particularly SGWs, is the goal of this research in order to demonstrate how well these techniques handle noisy remotely sensed data. The topic of spectrum noise elimination is covered in detail (Fan et al., 2007; Cao et al., 2005). The sensitive IMF with fault information is crucial for speeding up processing once the signal has been decomposed. The correlation coefficientbased sensitive IMF selection method that has been proposed. The defective signal is then reconstructed via the faulty IMFs, which are found using the TSK. An enhanced method and its use in planetary gearbox problem diagnosis are examined in this research. (EEMD), kurtosis and (SGW) are the foundations of the hybrid approach that is suggested.

Our paper's strategy is as listed below:

Section 2 provides a brief overview of the basic concepts of EEMD, SGW, and time-spectral kurtosis (TSK). The Signal analysis procedure is briefly presented in Sec.2. In Sec. 4, the frequencies of vibration features are provided, and Sec. 5 displays the experimental setup. The research results validate the effectiveness of the suggested approach in Sec. 6. Lastly, the paper is concluded in Sec. 7

BRIEF OVERVIEW OF THE BASIC CONCEPTS OF SGW, EEMD AND (TSK).

The denoising procedure

Second-generation wavelet (SGW) is a new wavelet model that has appeared in latest years. The development of SGW circumvents the Fourier transform, unlike the traditional wavelet (Gleich et al., 2010; Na et al., 2016). Vibration data from bearings and gears are denoised and features are extracted using this technique. Figures1 illustrate principle of SGW transform.

1) Divide: the signal $Y = \{y[m], m \in Z\}$ separated into the odd sample $Y_0 = \{y_0[m], m \in Z\}$ and the even sample set $Y_e = \{y_e[m], m \in Z\}$

$$y_0[m] = y[2m+1] (1)$$

$$y_e[m] = y[2m] \tag{2}$$

2) Use the prediction operator $Q(X_e)$ to estimate Y_0 on the even sample. Next, the estimate error between $y_0[m]$ and $Q(X_e)$ reveals E[m]:

$$E[m] = x_0[m] - Q(X_e) \tag{3}$$

3) The detail coefficients E = {e[m], m ∈ Z} can be updated by using the update operator V. then add the result V(E) to y_e[m]; the approximation coefficients f[m] can be achieved:

$$f[m] = y_e[m] + V(E) \tag{4}$$

- 4) Following the three procedures mentioned above, the detail coefficients $E = \{e[m], m \in Z\}$ and the approximation coefficients $F = \{f[m], m \in Z\}$ are achieved.
- 5) By repeating these three stages SGW is realizable. The prediction operator in this case $Q = [q(1), q(2), \ldots, q(M)]$ and update operator $V = [v(1), v(2), \ldots, v(N)]$.

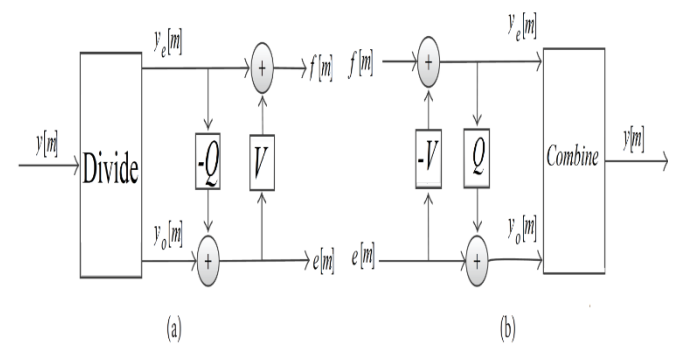


Fig. 1. SGW method; (a). SGW decomposition, (b). SGW reconstruction.

6) The interpolation subdivision method can be used to design them and the reconstruction phase of SGW is the reverse approach.

Decomposition procedure

In order to decompose signal (S_t) into Intrinsic Mode Functions (IMFs), Huang et al. introduced EMD as an adaptive signal analysis methodology (N. E et al., 1998; P. Flandrin et al., 2004).

The following characteristics are met by any IMF:

- 1) The maximum difference between the number of local extrema and zero-crossings is one.
- 2) An IMF's upper and lower envelope means values, which are determined from local maxima and minima, are always zero.

Input: $S_t = \{x_1, x_2, ... x_t\}$, limit of the cessation condition ε (usually fixed in [0.2; 0.3] Phase of decomposition:

1. Set n=1 then $r_0(t)=S_t$.

2. Excerpt IMF n(t):

Pseudo code for EMD decomposition.

- a. Set: $d_m(t) = r_{n-1}(t)$, while m = 1.
- b. Find the local maxima and minima of $d_m(t)$, $W_m(t)$ and $Z_m(t)$, correspondingly.
- c. Calculate the envelope: $A_m(t) = (W_m(t) + Z_m(t))/2$
- d. Make the novel element $d_{m+1}(t)$ of the following sifting iteration:

$$d_{m+1}(t) = d_m(t) - A_m(t)$$
 (5)

e. Use the following formula to determine the difference in squares between two successive siftings:

$$T(j) = \sum_{l=1}^{t} \frac{|d_{m+1}(z) - d_m(z)|^2}{|d_m(z)|^2}$$
 (6)

- f. When the ending condition $T(m) < \varepsilon$ is confirmed, the novel $IMF_n(t) = d_{m+1}(t)$ is described then proceed to Step 3; If not, follow Steps 2.b through 2.f to repeat a sifting cycle then update m = m + 1.
- 3. The residue should be updated in the following approach: $r_n(t) = r_n(t) IMF_n(t)$
- 4. The decomposition procedure terminates when there are less than two extrema in $r_n(t)$ or if $r_n(t)$ is monotone; if not, perform Step 2 using n = n + 1.

The initial time series x_t is decomposed by the procedure of sifting into:

$$S_t = \sum_{n=1}^R IMF_n(t) + r_R(t) \tag{7}$$

EMD is hampered by mode-mixing, a phenomena in which nearly identical oscillations persist in different IMFs. EEMD has been developed in order to solve these issues. Using an ensemble of IMFs by adding a white Gaussian noise is the fundamental concept of EEMD. By using the hybrid filter bank of the EMD, the impact of including white Gaussian noise lessens the mode-mixing issue. (P. Flandrin et al., 2004).

Pseudo code for EEMD decomposition

Input: $S_t = \{x_1, x_2, ... x_t\}.$

Output: A set of ensemble $IMFs\{\overline{IMF_n}(\Lambda)\}$,

$$(n = 1,2,...,R; m = 1,2,...,M)$$

1. Create the time series with noise:

$$S_n^m = S_t + b_n^m, m = 1, 2, ..., M$$

With M is the predetermined number of noise realizations and b_n^m realizations of white Gaussian noise.

- 2. For each time series S_n^m , execute 1 to get the corresponding $\{IMF_n(t)\}$, (n = 1,2,...,R; m = 1,2,...,M)
- 3. Average the $IMF_n(t)$ to estimate $\overline{IMF_n}(\Lambda)$:

$$\overline{IMF_n}(t) = \frac{1}{M} \sum_{m=1}^{M} IMF_n^m(t)$$
 (8)

The initial time series S_t is decomposed by the EEMD to R IMFs plus a residue:

$$S_t = \sum_{n=1}^R \overline{IMF_n}(t) + r_R(t) \tag{9}$$

After the signal has been decomposed, the sensitive IMF containing fault information is essential to accelerating processing. The suggested sensitive IMF selection technique based on correlation coefficients is as follows:

Determine the kurtosis value using the formula below:

$$R_n = \frac{1}{M} \sum_{n=1}^{M} \left(\frac{x_n - \bar{x}}{\beta} \right)^4 \tag{10}$$

Where \tilde{x} , β , M, and x_n are average values, the signal's standard deviation, the number of samples and the signal's specific (P. Nguyen et al., 2016).

The level of correlation between two signals can be calculated using the correlation coefficient (CC) by:

$$CC = \frac{\sum_{n=0}^{M} (x_n - \bar{x})(y_n - \bar{x})}{\sqrt{\sum_{n=0}^{M} (x_n - \bar{x})^2 (y_n - \bar{x})^2}}$$
(11)

In this case, y_n and \tilde{y} are the signal's particular and average values [24]. The precision of the reconstructed signal may be impacted by the end effect of the EEMD process, which can result in certain undesired IMFs, particularly at lower frequencies. A lower value suggests that the IMF's assistance was negligible, therefore are taken out before the reconstruction (Wang et al., 2016).

Time-spectral kurtosis (TSK)

The TSK is used to precisely identify the gear fault after the shaft IMFs have been eliminated. It is independent of time information and depends only on the statistical distribution of amplitude series. Defective signals really show up in vibration signals on a periodic basis. The defective signal is then reconstructed via the faulty IMFs, which are found using the TSK (Antoni et al., 2006; B. Chen et al., 2014). Because of its ability to tolerate sparse interference impulses, the TSK approach is used to adaptively determine resonance, as specified by:

$$TSK(k,f) = \frac{|(\hat{G}(m,f),|Y_{\text{STFT}}(k,f)|)|^4}{|(\hat{G}(m,f),|Y_{\text{STFT}}(k,f)|)|^2} - \frac{|\hat{G}(m,f)|^4}{|\hat{G}(m,f)|^2}, \ f \neq 0$$
(12)

The calculated Gaussian series, $\hat{G}(m, f)$ is derived from the initial signal's STFT amplitude series $|Y_{\text{STFT}}(k, f)|$. By looking for the TSK's highest peak, we can identify the resonance. In accordance with this, the fault IMFs for the fault signal reconstruction is selected from the resonance band. The following succinctly describes detailed TSK.

First, the raw vibration signal's STFT is computed.

Step 2: Entropy for the STFTAS is used to preprocess the outliers.

Step 3: Preprocessed STFT are used to estimate the Gaussian component $\hat{G}(m, f)$. First, the STFT amplitude series mean value is determined. Next, choose points whose amplitude is smaller than the n-times mean, and use these points to create a new series. The goal series with an approximate Gauss distribution can

be generated by a number of iterative calculations.

Step 4: Using |Y(k, f)| and G(m, f), the TSK value of the k-th frame signal at frequency f is determined using Equation (12).

Step 5: The TSK value is used to design the filter H(k, f)

$$H(k,f) = \begin{cases} 1 & \text{TSK } \ge \text{ Threshold} \\ 0.01 & \text{TSK } < \text{ Threshold} \end{cases}$$
 (13)

Step 6: Reconstructing the signal by multiplying the STFT values by H(k, f).

Step 7: The Hilbert transformation is used to demodulate the reconstructed signal.

The signal analysis algorithm

Gear damage diagnosis is an extremely challenging endeavor. This study combines the SGW and EEMD algorithms to identify the defect feature frequency of weak gear signals. The numerical approach's steps are clarified below:

Step 1: Filtering the original signal and extracting the signal of interest from the noise using SGW denoising.

Step 2: Apply the EEMD technique to suppress modal aliasing and decompose the purified signal into IMFs.

Step 3: To choose the best IMF components, timespectral kurtosis (TSK) and correlation coefficient of each IMF are then determined.

Step 4: Lastly, the characteristic frequency is achieved through envelope spectrum analysis. The signal analysis procedure appears in Fig. 2 and MATLAB is employed for analyzing the data collected.

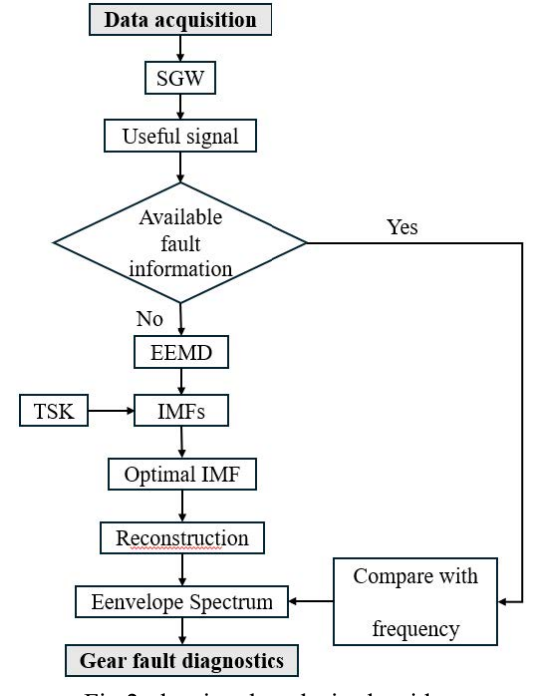


Fig.2. the signal analysis algorithm

Expérimental Test Setup

A straightforward test rig is employed to illustrate the study conditions and gauge the effectiveness of the suggested methodology in order to ensure its efficiency and reliability. As shown in Figure 3 a (3KW) asynchronous drive motor in three phases powers the gearbox. A magnetic powder brake is employed to supply load, and speed and torque sensors are used to obtain the speed and torque data. These parts are joined by couplings. investigational system has a 12,800 Hz sampling frequency. Additionally, 6.5 Nm and 13.5 Nm are the corresponding loads that are regulated by a controlled magnetic brake mechanism. Schematic figure of a planetary gearbox and its dynamical model is exposed in Fig. 4. Fig. 6 illustrates the arrangement of the planetary gearbox's sensors. The damaged gear is displayed in Figures 7, respectively.

The corresponding feature frequency is linked to the rotating speed of the defective gear in relation to the planet carrier, also when a planetary gearbox has a tooth deficiency, the vibration signal experiences significant modulation characteristics and periodic shocks. Equations (14) and (15) are used to calculate the planetary gearbox's characteristic frequencies (Qiang et al., 2015). while Table 1 contains a list of them.

$$f_{\omega} = f_n - f_d = f_d \frac{N_r}{N_n} \tag{14}$$

$$f_h = N_r f_c = N_p (f_d + f_p) = N_n (f_n - f_d)$$
 (15)

N_n: sun gear's teeth number

Nr: ring gear's teeth number

N_p: planet gear's teeth number

f_n: frequency of sun gear

fd: frequency of carrier

fp: frequency of planet gear

F_h: frequency of meshing

 f_{ω} : the sun gear's frequency in relation to the carrier

Table 1. Frequency parameters of the planetary gearbox.

Fn	F_d	F_{ω}	F_h
16.42	4.85	11.57	300.82

Results and discussions

The appearance of periodic impulse components in vibration signals is a crucial indicator of gear failure in the diagnosis of gear faults. However, it is challenging to recover the weak periodic impulse patterns due to the high background noise. Figures (7-a) and (7-b) display the time domain of a typical gear and a broken gear.

Nevertheless, these features are obscured by noise and are not noticeable enough to identify the

presence of defects. Time-frequency representations (Figures (8-a) and (8-b)) demonstrate that the frequency of the normal gear resides in the low-frequency band, while the cracked gear's frequency is focused in the high frequency band. Figures (9-a) and (9-b) show the frequency domain of the gear failure. However, the fault's associated frequency is obscured, which is unable to discern the periodic pulse characteristics. making it difficult to find fault diagnostic information using the time and frequency domains. Consequently, the present research offers a potential defect identification approach for gears based on EEMD, SGW, and kurtosis to identify periodic impulse properties.

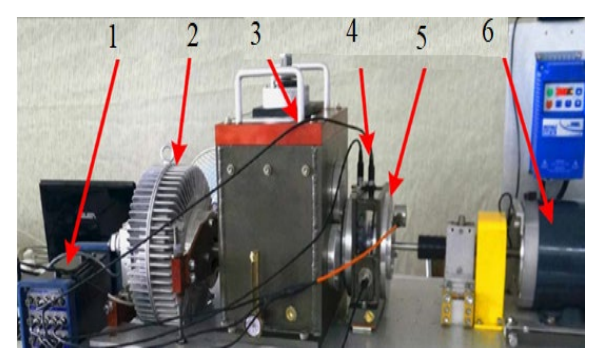


Fig. 3. Planetary gear fault test (1) Data acquisition system, (2) load system(3) fixed-axis gearbox, (4) vibration sensors, (5) planetary gearbox, (6) Drive motor.

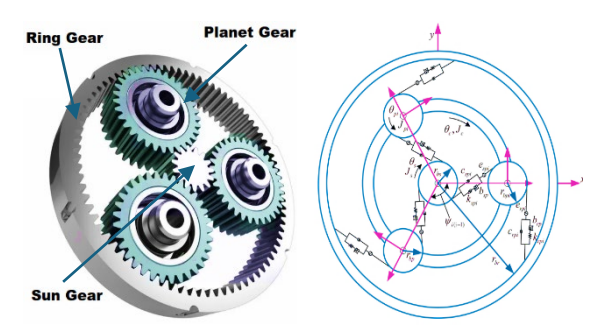


Fig. 4. (a) schematic figure of a planetary gearbox, (b) dynamical model



Fig. 5. vibration sensors



Fig. 6. damaged gear

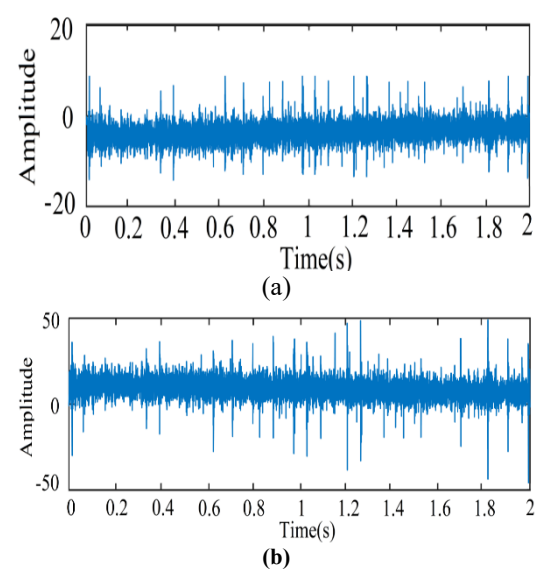


Fig. 7. Time domain of (a) normal gears, (b) broken gears.

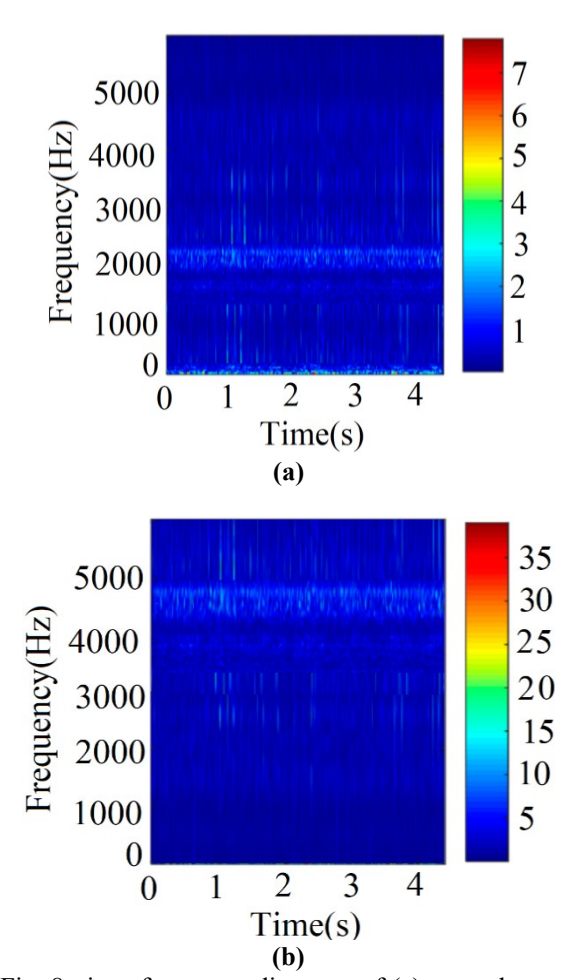


Fig. 8. time–frequency diagrams of (a) normal gears, (b) broken gears.

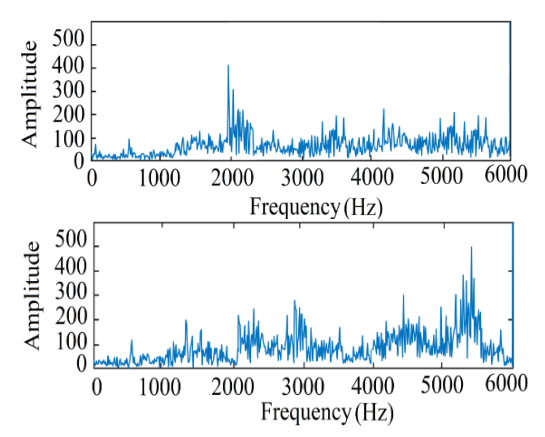


Fig. 9. Spectrum of (a) normal gears, (b) broken gears.

To enhance the denoising impact of the vibration signal, a second-generation wavelet (SGW) denoising approach has been offered; the results can be seen in Fig. 10, from which we observe that noises are significantly decreased while the legitimate signal amplitude is completely preserved. As a result, we may infer that the suggested method produces the best denoising performances.

For the purpose of showing the success of the suggested technique, the signal that was collected is decomposed using EEMD. As shown in Fig. 11, the EEMD approach can decompose non-stationary vibration signals including failures in a sum of stationary component IMFs, which has the benefits of eliminating mode mixing.

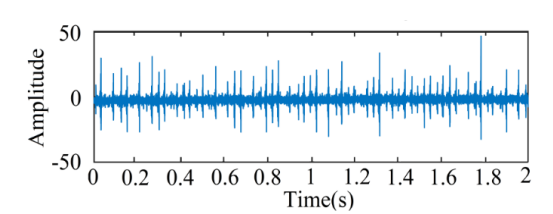


Fig. 10. Denoising by SGW technique

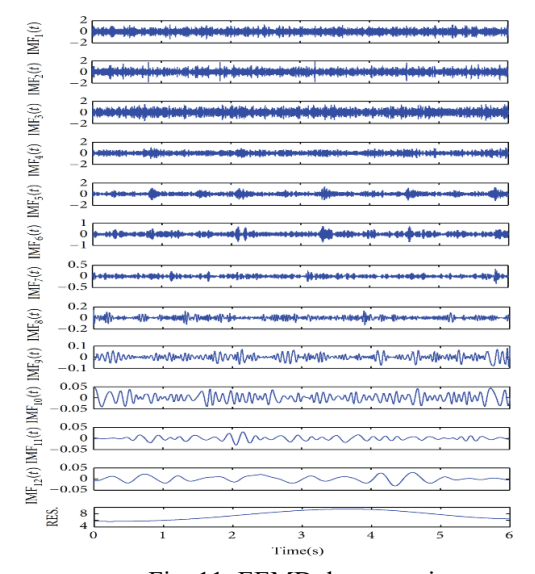


Fig. 11. EEMD decomposing

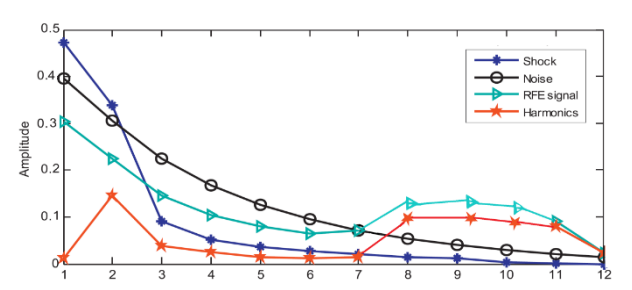


Fig. 12. The (CC) associated with the IMFs and the RFE.

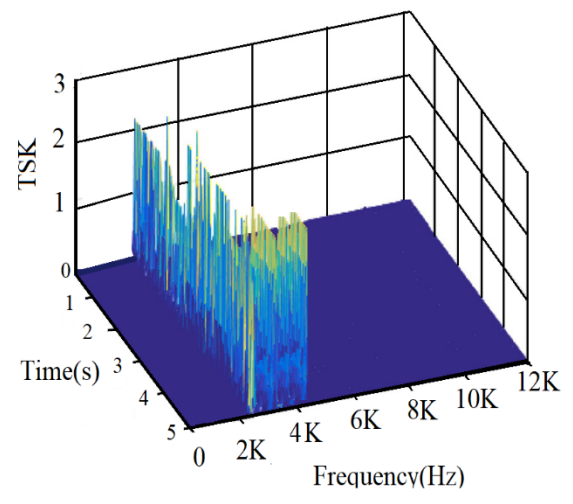


Fig. 13. The time-spectral kurtosis

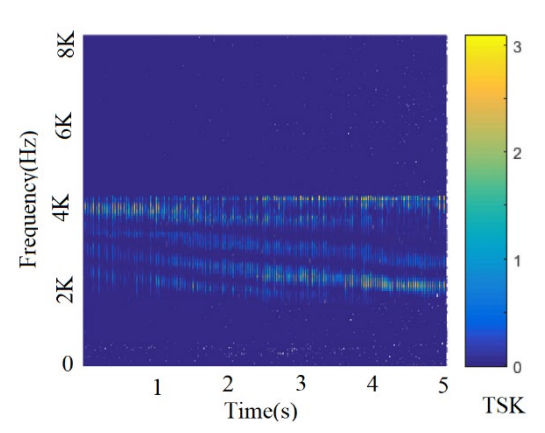
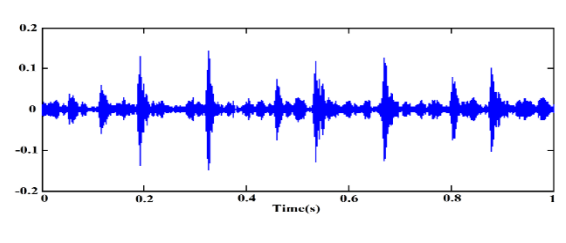


Fig. 14. The two-dimensional view

Knowing that the most important components of the signal are, the background noise, harmonic contributions and a series of fault induced impulses. To identify the ideal IMFs, the (CC) associated with the IMFs and the reference signals RFE are displayed. Through the operation of EEMD, the signal is divided into 12 IMFs. Figure 11 shows that when the decomposition level increases, the highest values of the (CC) drop, as well as the IMF1, IMF2, and IMF3 are considered to signal reconstruction. We can also check this by using TSK in Fig. 13. It is evident that the frequency range of 2.3–4.2 kHz is about where the resonance caused by the fault appears. therefore, we will chooseIMF1, IMF2 and IMF3 as fault IMFs.

Additionally, we can see that more clearly in the twodimensional view as shown in Fig. 14.

A gearbox's vibration signal is made up of a variety of factors, including rotational frequency, so is not just caused by vibrations in the gear meshing. Typically, the gear meshing frequency will be high relative to the shaft rotation frequency, which appears in the low frequency region. In Fig.15 the meshing frequency and the sidebands are evidently discovered. These characteristic frequencies are indicating damages occurring in the planetary gearbox. Moreover, the value of the sidebands is almost equal to the rotating frequency of the sun gear, which suggests the damage on the sun gear in planetary gearbox. It agrees to the value shown in the Table 1. Correspondingly, background noise is effectively decreased since the EEMD filtering order is from high frequency to low frequency. Hence, these results can guarantee that the chosen IMFs include details of gear faults. We deduce that the suggested approach can successfully identify the planetary gearbox's defects.



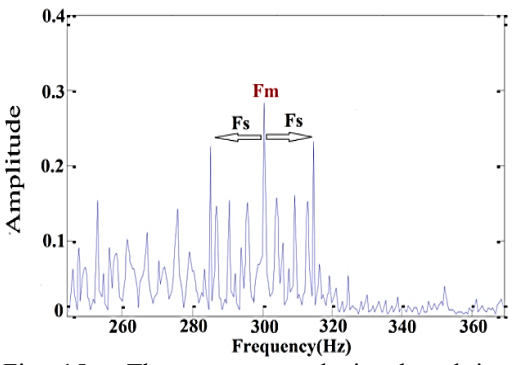


Fig. 15. The reconstructed signal and its Zoom spectrum

Conclusions

This work proposes an adaptive strategy to address the challenge of weak feature extraction in planetary gearbox malfunction diagnosis. different concepts can be used to describe the main effects on this work. In order to separate the signal of interest from the background noise, SGW denoising is first used to filter the original signal. After that, decompose the filtered signal into IMFs and use the EEMD technique to reduce modal aliasing. The best IMF components are then chosen by calculating correlation coefficient and time-spectral kurtosis (TSK). Finally, the characteristic frequency is determined by analyzing the reconstructed signal's envelope

spectrum. We conclude that the proposed method can effectively detect defects in the planetary gearbox and we hope that the research will assist researchers and experts in efficiently applying current damage detection algorithms and creating more dependable and useful techniques in the field of fault diagnosis.

ACKNOWLEDGMENT

The authors would like to gratefully acknowledge Higher Normal School of Technological Education of Skikda, Algeria; for their support of this research

REFERENCES

- Amarnath, M., Krishna, I.P., "Empirical mode decomposition of acoustic signals for diagnosis of faults in gears and rolling element bearings," *IET. Sci. Mea.Technol*, No 279-287(2016).
- Antoni, J., Randall, R. B., "The spectral kurtosis: application to the vibratory surveillance and diagnostics of rotating machines," *Mechanical System and Signal Processing*, No 20, 308-331(2006).
- B. Chen, Z.L. Yan, W. Chen, "Defect Detection for Wheel-Bearings with Time-Spectral Kurtosis and Entropy," *Entropy* No 16 607–626(2014).
- Braun, S., "Mechanical Signature Analysis", *Academic Press, London*, (1986).
- Cao, S., Chen, X., "The second-generation wavelet transform and its application in denoising of seismic data," *Appl. Ge-ophys*, No 2: 70–74(2005).
- Cheng, J., Yu, D., Tang, J., Yang, Y., "Application of frequency family separation method based upon EMD and local Hilbert energy spectrum method to gear fault diagnosis," *Mech. Mach. Theory*, No 43, 712–723(2008).
- Dragomiretskiy, K., Zosso, D., "Variational mode decomposition," *IEEE Trans. Signal Processing*, No 62, 531–544(2014).
- Elforjani, M., Bechhoefer, E., "Analysis of extremely modulated faulty wind turbine data using spectral kurtosis and signal intensity estimator," *Renew. Energy*, 127, 258–268(2018).
- Fan, X., Liang, M., Yeap, T. H., Kind, B., A "joint wavelet lifting and independent component analysis approach to fault detection of rolling element bearings," *Smart Materials and Structures*, No 16 (5): 1973–1987 (2007).
- F. Li., B, Zhang., S. Verma., K.J. Marfurt., "Seismic signal denoising using thresholded variational mode decomposition," *Exploration Geophysics*, No 49 (4), 450–461(2018).
- Gleich, D., Kseneman ,M., Datcu ,M., "Despeckling of terraSAR-X data using second-generation

- wavelets," *IEEEGeosci Remote Sens Lett*, No 7(1):68–72(2010).
- Iatsenko, D., P.V. McClintock., A. Stefanovska., "Nonlinear mode decomposition: a noiserobust, adaptive decomposition method," Physical Review, No 92 (3),032916(2015).
- J. Pan., J. Chen., Y. Zi., Y. Li., Z. He., "Monocomponent feature extraction for mechanical fault diagnosis using modified empirical," Mech. Syst. Signal Processing, No 20, 108-122(2008).
- Lei, Y., Yang, B., Jiang, X., Jia, Li, F., Nandi, N., A.K., "Applications of machine learning to machine fault diagnosis: A review and roadmap," *Mech. Syst. Signal Processing*, No 138, 106587(2020).
- L. Hui., Y. Zhang., and H. Zheng., "Wear detection in gear system using Hilbert-Huang transform," *Journal of Mechanical Science and Technology*, No 20,11,1781–1789(2006).
- Na, Lu, Guangtao, Zhang., Yuanchu, Cheng., Diyi, Chen., "Signal Denoising Method Based on Adaptive Redundant Sec-ond-Generation Wavelet for Rotating Machinery Fault Diagnosis," *Mathematical Problems in Engineering*, No 3(2):39–45(2016).
- N. E., Huang et al., "The empirical mode decomposition and the Hilbert spectrum for nonlinear and non-stationary time series analysis," *Proc. R. Soc. A Math. Phys. Eng. Sci.* No 6(1):22–30(1998).
- P. Flandrin., G. Rilling., P. Goncalves., "Empirical mode decomposition as a filter bank," *IEEE Signal Process. Lett*, No 2,112–114(2004).
- P. Nguyen, J. M. Kim., "Adaptive ECG denoising using genetic algorithm-based thresholding and ensemble empirical mode decomposition," *Inf. Sci. (Ny)*, No 6, 679-698(2016).
- Qiang, Miao., Qinghua, Zhou., "Planetary G earbox Vibration Signal Characteristics Analysis and Fault Diagnosis," *Shock and Vibration*, No 2, 712–723(2015).
- Qin, Y., Mao, Y., Tang, B., Wang, Y., Chen, H., "Mband flexible wavelet transform and its application to the fault diagnosis of planetary gear transmission systems," *Mech. Syst. Signal Processing*, 134, 106298(2019).
- S. Chen., Y. Yang., Z. Peng., X. Dong., "W. Zhang., G. Meng. Adaptive chirp mode pursuit. Algorithm and applications," *Mechanical Systems and Signal Processing*, No 116, 566–584(2019).
- Smith, J. S., "The local mean decomposition and its application to EEG perception date," *JR Soc interface*, No 2(5):443-454(2005).

- Ta., Jen, Peng. Ping., H.K. Wei. C., Cheng. Ch.W., "Nonlinear Dynamic Analysis and Forecasting of Symmetric Aerostatic Cavities Bearing Systems," *International Journal of Bifurcation* and Chaos, No 04 (34), 2430008 (2024).
- Upadhyay, A., Pachori ,R., "Speech enhancement based on memd-vmd method," *Electronics Letters* No 53 (7) 502–504(2017).
- Wang., C. Kuo., P. Peng., Ta. Oshima., M. Chen., Y., "Voting Model Prediction of Nonlinear Behavior for Double Circumferential-Slot Air Bearing System," *Chaos Solitons & Fractals. Elsevier*, vol. 183(C), 114908 (2024).
- Wang, Y., Xiang, J., Richard, M., "Spectral kurtosis for fault detection, diagnosis and prognostics of rotating machines," A review with applications.

 Mechanical Systems and Signal Processing, No 66, 679-698(2016).
- Yu, G., "A Concentrated Time-Frequency Analysis Tool for Bearing Fault Diagnosis," *IEEE Trans. Instrum. Meas*, No 69, 371–381(2020).
- Z. P. Feng and F. L. Chu., "Transient hydraulic pressure fluctuation signal analysis of hydroturbine based on Hilbert-huang Transform," *Proceedings of the CSEE*, No 10,111–115(2005).